

UNRAVELLING PETROFABRICS IN THE BRECCIATED CM CHONDRITE COLD BOKKEVELD

C. J. Floyd¹, A. Macante², L. Daly^{1,3,4} and M. R. Lee¹, ¹School of Geographical and Earth Sciences, University of Glasgow, G12 8QQ, UK (C.floyd.1@research.gla.ac.uk), ²Department of Civil and Environmental Engineering, University of Strathclyde, G1 1XJ, UK, ³Australian Centre for Microscopy and Microanalysis, The University of Sydney, Sydney, NSW, Australia, ⁴Department of Materials, University of Oxford, Oxford, UK

Introduction: Impacts are thought to have had a significant role in shaping and altering C-complex asteroids during their early evolution. The best evidence for such shock processing is preserved as brecciation and petrofabrics which can be observed throughout the CM carbonaceous chondrites in both 2D and 3D [1-6]. The presence of petrofabrics within the CM chondrites that simultaneously exhibit little to no evidence of shock in the microstructures of their silicate minerals (most typically classified as S1 [2]), has led authors to suggest that petrofabrics formed by multiple low-intensity impacts [2]. Continued analysis of these petrofabrics can provide insights into the scale and chronology of the deformation experienced on the CM chondrite parent body/ies. In this study we use 3D petrofabric analysis to investigate the deformation history of the CM chondrite Cold Bokkeveld.

Methods: X-ray computed tomography (XCT) was carried out on a 2.154g chip of Cold Bokkeveld, a brecciated carbonaceous CM chondrite which fell in 1838 and has been classified as having a range of petrological subtypes from CM2.1-2.7 [7,8]. XCT was conducted at the University of Strathclyde using an XT H320 LC instrument equipped with a 180 kV transmission source, producing a 3D volume with a final reconstructed voxel size of 11.15 μm .

At least 15 lithologies were identified within the reconstructed volume by differences in X-ray attenuation, with three spatially separated lithologies (L_1 , L_2 , L_3) were selected as the focus of this study. Within L_1 , L_2 and L_3 a total of 125 dark-toned objects were identified as chondrules [3], alongside 53 bright objects within L_1 classified as metal grains [9]. Identified chondrules and metal grains were manually segmented using the method set out in [3] with a representative cross-section segmented in each orthogonal plane (XY, XZ and YZ). Segmented planes were subsequently imported into BLOB3D [10] where a specialized merit function was used to fit an ellipsoid to the segmented sections. Directional cosines of the ellipsoids long and short axes were transformed into trend and plunge and plotted on stereographic projections using Stereonet10 software [11].

Results: Chondrule Orientations: Within all three lithologies chondrules are observed to have preferred orientations; their long axis orientations plot along great circle girdles, and their tertiary axis orientations clustering. Such trends are indicative of a foliation fabric (Fig

1). This interpretation is supported by shape parameter K (Table 1) where $K < 1$ indicates a girdle distribution and $K > 1$ indicates a cluster distribution [12]. The strength of the fabrics is indicated by strength parameter C (Table 1), where $C = 0$ indicates a weak fabric, $C = 2$ a moderate fabric and $C > 4$ a strong fabric [3, 12]. The distributions of L_1 , L_2 and the long axis of L_3 are non-random at the 99% confidence interval (CI) whilst the L_3 short axis is non-random at 97.5% CI. Analysis of the long axis third eigenvector for each lithology indicates a foliation orientation difference of $L_1: L_2 = 8.7^\circ$, $L_2: L_3 = 27.3^\circ$, $L_1: L_3 = 18.6^\circ$.

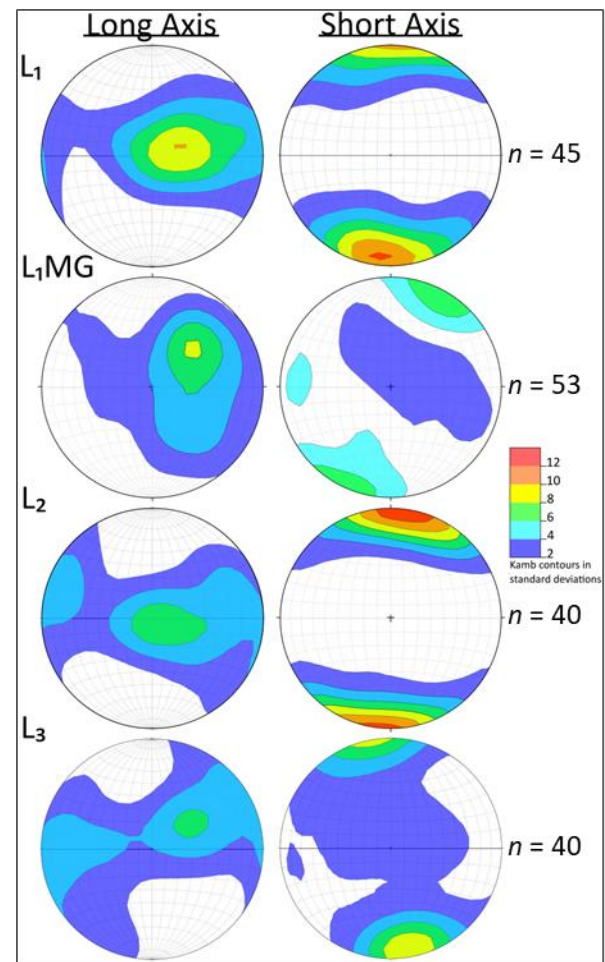


Figure 1. Equal area stereographic projections of the long and short axes of chondrule best fit ellipsoids within the three lithologies (L_1 , L_2 , L_3) and metal grain best fit ellipsoids within the L_1 lithology ($L_1\text{MG}$).

Metal Grain Orientation: In addition to containing chondrules, lithology L₁ was also observed to contain numerous metal grains. They were segmented and analysed to investigate potential differences in orientation between the silicate and metallic components of the same lithology, which if present would be significant as both components should have been subjected to similar processing. The results are displayed in Fig 2. and show clustering of both the long and short axes, indicating a lineation (Table 1). This conclusion is supported by the *K* parameter calculation, with the *C* parameter indicating that this is a weak lineation. The metal grain distribution is found to be non-random at a CI of 97.5% for the long axis and 99% for the short axis.

Table 1. Orientation shape (*K*) and strength (*C*) parameters for the chondrules and metal grains analysed in L₁, L₂ and L₃.

Component	Long Axis		Short Axis	
	K	C	K	C
L1	0.671	1.938	1.791	1.913
L1MG	54.935	0.843	1.545	0.854
L2	0.269	1.458	1.727	2.145
L3	0.197	1.065	1.779	0.940

Shape Analysis: Particle shape analysis was carried out on the produced ellipsoids using Sneed and Folk diagrams [13]. Across all three lithologies chondrules have shapes sitting predominantly across the compact bladed/compact elongate shape ranges, with some falling within the compact shape region. Conversely metal grains within L₁ had a dominantly compact shape (37.71%).

Discussion: The data presented here indicate that three lithologies within Cold Bokkeveld contain weak-moderate chondrule defined petrofabrics. The fabric strengths recorded here are weaker than those observed in Murchison (CM2.5) [3, 7] but greater than in Aguas Zarcas (brecciated CM2) [5,14]. The foliation orientation is broadly consistent between L₁ and L₂ and shows a slight difference in direction between L₁/L₂ and L₃ suggesting a possible subtle variation in L₃ chondrule orientation. The similarities in observed foliation orientation and strength between L₁, L₂ and to a lesser extent L₃, despite being spatially separated within the 3D volume, suggest that all three fabrics were imposed concurrently. The implication of this finding is that a period of petrofabric inducing shock processing followed aqueous alteration and brecciation. Further data collection to better constrain orientations differences is needed, especially with respect to the long axes. Regardless, this trend indicates that care should be taken when discussing the relationship between petrofabric shape/strength

and the extent of aqueous alteration as described by [15]. Careful assessment of potential differences in petrofabrics between lithologies is needed to allow accurate determination of event chronology.

Differences in the L₁ metal grain fabric shape, strength, and orientation relative to the L₁ chondrules (lineation as opposed to foliation) suggests the metallic components may be reacting differently in response to fabric forming impacts. Differences may be the result of deformation around the L₁ chondrules causing a deflection in their preferred orientations [16].

Conclusion: The results presented here show that three lithologies within CM chondrite Cold Bokkeveld have definable petrofabrics when analysed using XCT. The observed similarities in the orientations of these fabrics suggest that petrofabrics developed after aqueous alteration and brecciation, hinting at impact processing and fabric development occurring throughout the entire history of the parent body and not just in the period prior to aqueous alteration. Additionally, evidence from the L₁ metal grain orientations suggests that they may be reacting/recording impact induced fabrics differently to chondrules

Acknowledgments: XCT data acquisition and processing were supported by the Oil & Gas Innovation Centre at the university of Strathclyde. I would also like to thank; SAGES for the small grant which allowed this data to be collected The Natural History Museum (UK) for the chip of Cold Bokkeveld, STFC for funding this research and Pierre-Etienne Martin for his helpful thoughts on this work.

References:

- [1] Bischoff A, et al., (2006) *Meteorites and the Early Solar Sys. II*, 679-712
- [2] Lindgren P et al., (2015) *Geochim. Cosmochim. Acta*, 148, 159-178
- [3] Hanna R, D et al., (2015) *Geochim. Cosmochim. Acta*, 171, 256-282
- [4] Jenkins L, E et al., (2021) *84th Annual Meeting of the Met. Society*, #2609
- [5] Floyd C, J et al., (2022) *LPSC LIII*, #1470
- [6] King A, J et al., (2022) *Science Adv.* 8, [7] Rubin A, E et al., (2007) *Geochim. Cosmochim. Acta*, 71, 2361-2382
- [8] Lentfort S, et al., (2021) *Meteorit. & Planetary Sci.*, 1, 127-147
- [9] Friedrich J, M (2008) *Earth and Planetary Sci. Letters*, 275, 172-180
- [10] Ketcham R, A (2005a) *Geosphere*, 1, 32-41
- [11] Cardozo N & Allmendinger R, W (2013) *Computers and GeoSciences*, 51, 193-205
- [12] Woodcock N, H & Naylor M, A (1983) *J. of Structural Geology*, 5, 539-548
- [13] Sneed E, D & Folk R, L (1958) *J. of Geology*, 66, 114-150
- [14] Garvie L, A, J (2021) *American Mineralogist*, 106, 1900-1916
- [15] Rubin A, E (2012) *Geochim. Cosmochim. Acta*, 90, 181-194
- [16] Passchier, C, W (1982) *J. of Structural Geology*, 4, 69-79